Simulation of bioelectric potential changes in the styles of lilies using nerve impulse transmission models

Report no. WD 84-02

Simulation of Bioelectric Potential Changes in the Styles of Lilies using Nerve Impulse Transmission Models

R.M.M. Mattheij, J. Molenaar,
G.W.M. Staarink, E.W.C. van Groesen

February 1984

Project no. 830201

Wiskundige Dienstverlening
Faculteit Wiskunde en Natuurwetenschappen
Katholieke Universiteit
6525 ED Nijmegen

Telefoon 080-558833 tst 3138/2986

Contents

§1. Introduction

In pistils of plants belonging to different genera diverse types of electrical responses after pollination are measured [9,14]. These phenomena resemble nerve impuls transmission in human and animal axons. They also show, however, some characteristic features, which need further theoretical and experimental investigation. Spanjers found that in lilies [15] the shape of the pulses depends on the stimulus presented. For example, the electrical responses after self- and cross-pollination were quite different. Furthermore, the velocities of the traveling electrical pulses appeared to be in the order of cm/h which is considerably slower than nerve impulse transmission (m/s).

In this report we try to appreciate the results in the context of models which are known to be reliable for nerve impuls transmission. In section 2 we start with a presentation and analysis of the Hodgkin-Huxley model, which allows for conclusions about the measured curve shapes. In the following sections we direct our attention to the velocity range observed in plants. In this we found it more appropriate to use the simpler Fitzhugh-Nagumo model (section 3). In particular we study the influence of lignified cells near the vascular bundles on the membrane properties. In sections 4 and 5 we present two different approaches to this phenomenon. Firstly we assume membrane and lignified cells being indistinquishable. This allows for an application of the model without modifications. Secondly we treat membrane and lignified layer separately. In the latter case the model must be extended significantly and the calculations require more numerical effort. Conclusions drawn from both the theoretical analysis and the numerical calculations are given in section 6 together with suggestions for further research.

§2. The Hodgkin-Huxley model

The Hodgkin-Huxley (H.H.) model is frequently used to describe the electrical properties of nerves; for some results see e.g. [8,12,13]. In this model the nerve is assumed to be infinitely long, homogeneous in longitudinal direction and cylindrically symmetric in transversal direction. The nerve is embedded in a fluidal environment with negligible electrical resistance compared to the axoplasm resistance within the axon. To represent the system by an electrical circuit the nerve is divided into small identical compartments with length h (see figure 1). Within each compartment the membrane is replaced by a capacitance c_m parallel to a (non-linear) resistance R_m. The parts are connected by a resistance R_a, representing the longitudinal axoplasm resistance [7]. (See figure 2).

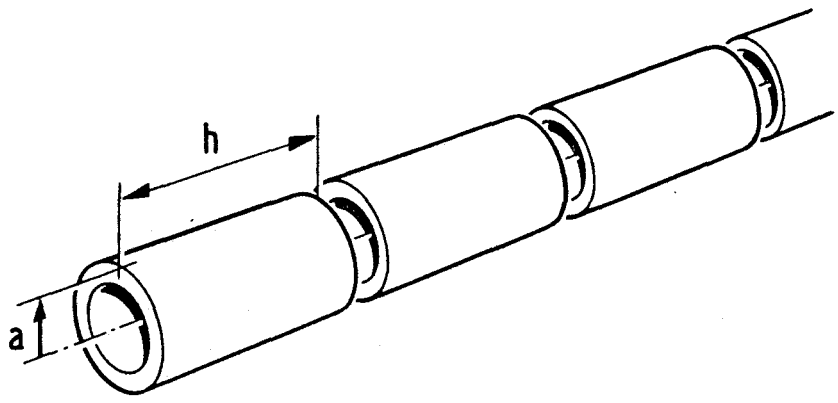

Figure 1. Division of the axon in compartments. The (mean) axon radius is denoted by a.

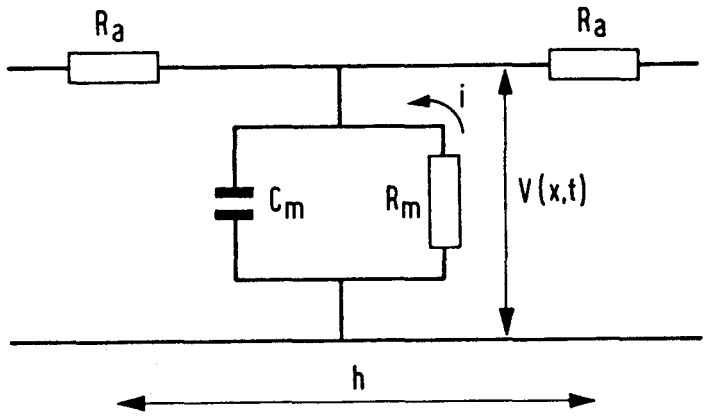

Figure 2. Representation of the axon by electrical components. The used symbols are dealt with in the text.

We are interested in the voltage V(x,t) over the membrane as a function of the position x along the nerve and time t. Application of Ohm's law yields the following partial differential equation for V.

$$\frac{1}{2\pi a R_a}\frac{\partial^2 V}{\partial x^2} = c_m \frac{\partial V}{\partial t} + i(V,m,n,h) \qquad (2.1)$$

R_a is the axoplasm resistance per unit length, c_m and $1/R_m$ are the capacitance and conductance of the membrane per unit area and a is the membrane radius. Membrane current per unit area is denoted by i. This membrane current is a complicated function of the voltage V, the sodium activation rate m, the potassium activation rate n and the sodium inactivation rate h, which in turn depend on V via differential equations. The latter equations together with equation (2.1) are refered to as the H.H. equations.

We now investigate how the electrical responses measured in lilies might be reproduced by means of the H.H. model. The measured signals are drawn in figure 3. In case of self-pollination a single traveling wave is found, whereas cross-pollination may lead to a peak directly followed by a broad plateau moving together with it.

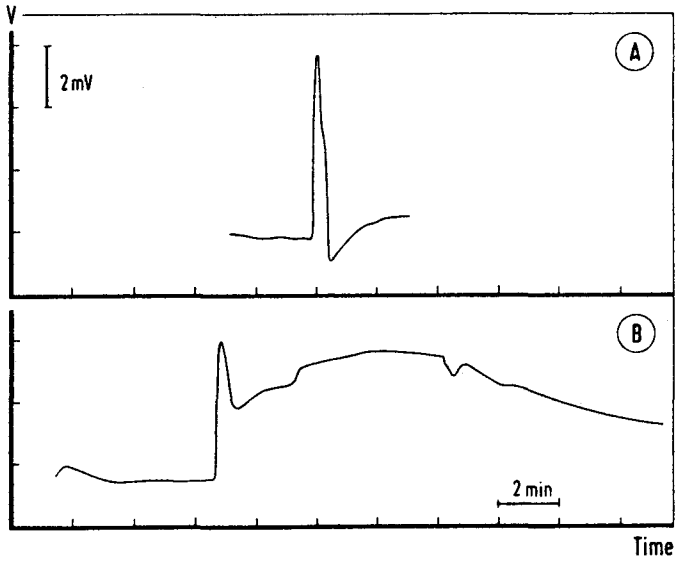

Figure 3. Examples of bioelectrical responses measured in the pistils of lilies. (a): The response after self-pollination; (b): the response after cross-pollination.

Carpenter [2] analyzed the possible solutions of a non-linear diffusion equation like equation (2.1) coupled with "fast" and "slow" differential equations. The "fast" ("slow") equations correspond to subprocesses whose rates are fast (slow) relative to the rate of the primary phenomenon. As for the H.H. model it is known that the equations for n and h have long timescales, whereas the m equation has a short timescale. It is shown that under mild qualitative conditions a set of equations like the H.H. equations may have traveling wave solutions, i.e. a wave which travels at a constant velocity and which returns to the rest state after the impulse has passed. The principal condition is that i(V,m,n,h) for fixed m,n,h is a cubic function of V.
It is well established that this condition holds in case of axons. Though not yet measured it is very likely that it holds in cases of vegetable membranes as well, because there the membrane conductance is controlled by similar processes.

In general the traveling wave solutions of the H.H. equations will have a single-pulse form just as is measured in the case of self-pollination (figure 3.a). If, however, the diffusion equation is coupled with two "slow" equations which differ considerably in timescale, then solutions with plateaus are admitted, which remarkably resemble the cross-pollination response given in figure 3b (cf. [4] and also figure 18 of [2]). So as for the shape of the measured curves the H.H. model seems to be applicable to vegetable membranes and it should be worthwhile to investigate the (in)activation mechanisms in detail.

§3. The Fitzhugh-Nagumo Model

In this section we direct our attention to the question why the electrical pulses in plants travel some orders of magnitude slower than they do in animal axons. For several reasons we prefer to introduce a simplified version of the H.H. model. Firstly, as already noticed earlier, the kind of subprocesses in the vegetable membrane are not well known. Secondly, in the following section we want to modify a known model in order to simulate lignification, which is a specific aspect of vegetable membranes. In the so-called Fitzhugh-Nagumo (F.N.) model [5, 11] all slow subprocesses are represented by one equation. The resulting set of equations still describes the typical membrane properties, but in an averaged manner. This implies, as shown by Carpenter [2], that the variety of solutions is less rich than in case of the H.H. model. For example, plateau solutions may not be expected within the F.N. model. Because we are here interested in the wave velocity this objection is of minor importance.

One obtains the F.N. model from the H.H. model in replacing the membrane resistivity R_m (see figure 2) by a two-branch circuit as drawn in figure 4.

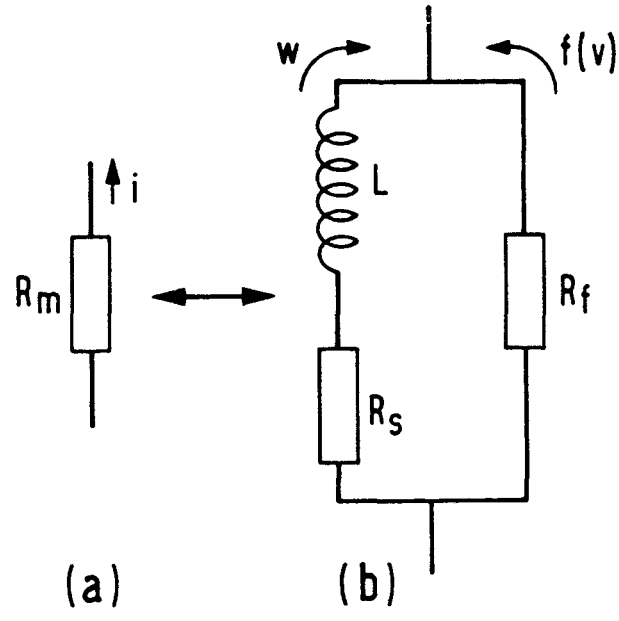

Figure 4. Please turn over for figure caption.

Figure 4.

In the F.N. model the membrane resistance R_m of the H.H. model (a) is replaced by a non-linear resistance R_f, only depending on the applied voltage, parallel to a series consisting of a coil with self-inductance L and a linear resistance R_s (b). The (L,R_s) branch represents all slow subprocesses, the R_f branch represents all fast subprocesses.

The branch consisting of an inductance L and conductance $1/R_s$ (both per unit area) simulates all relatively slow (in-) activation processes. One can control the "inertia" of this branch by adjusting the value of L. The current (per unit area) through these components is denoted by w. The effect of relatively fast processes is represented by the branch at the right hand side. The corresponding current f(V) (per unit area) is assumed to be a cubic function of the applied voltage V.
The partial differential equations of the F.N. model read in dimensional form as follows:

$$c_m \frac{\partial V}{\partial t} = \frac{1}{2\pi a R_a} \frac{\partial^2 V}{\partial x^2} - w - f(V)$$

$$L \frac{\partial w}{\partial t} = V - R_s w. \qquad (3.1)$$

Following an analysis by Fitzhugh [6] we can transform these equations into dimensionless form, thus reducing the number of parameters. The resulting equations are conveniently applicable to a whole class of similar systems. Let us introduce a fixed, arbitrarely chosen reference potential $\bar{V}$ and a parameter g defined by

$$g = \frac{df}{dV}\Big|_{V=V_R} \qquad (3.2)$$

The derivative is to be evaluated at the equilibrium potential V_R, which satisfies the condition

$$f(V_R) = -V_R/R_s. \qquad (3.3)$$

This condition for the steady state is obtained by setting in equation (3.1) all derivatices equal to zero. A suitable way to achieve the required transformation is to scale the used units according to the following substitutions:

$$\begin{aligned} &\text{time } t && \to t/(\frac{c_m}{g}) \\ &\text{length } x && \to x/(2\pi a\, R_a g)^{-\frac{1}{2}} \\ &\text{voltage } V && \to V/\bar{V} \\ &\text{current (per unit area) } w,f && \to w/g\bar{V} \ , \ f/g\bar{V} \end{aligned} \tag{3.4}$$

If confusion is hardly possible we use the same notations for dimensionless variables and functions and dimensional ones. Using the substitutions (3.4) we arrive at the dimensionless equations

$$\begin{aligned} \frac{\partial V}{\partial t} &= \frac{\partial^2 V}{\partial x^2} - w - f \\ \frac{\partial w}{\partial t} &= \varepsilon(V-\gamma w) \end{aligned} \tag{3.5}$$

The parameters ε and γ are given by

$$\varepsilon = (\frac{c_m}{g})/(gL) \qquad \text{(a)}$$

$$\gamma = gR_s \qquad \text{(b)} \tag{3.6}$$

From the notation used in equation (3.6a) we recognize that ε can be looked upon as the ratio of two time constants c_m/g and gL which are characteristic for the time scales of fast and slow ionic processes respectively. From this interpretation we immediately derive that the condition $\varepsilon << 1$ should hold. To estimate γ we notice from definition (3.2) that g is inversely proportional to the resistance of the fast branch at $V = V_R$. Because it is reasonable to assume that the membrane permeability, apart from different time scales, is nearly the same for all ionic currents, we use the approximation

$$g \approx R_s^{-1} \tag{3.7}$$

and consequently $\gamma \approx 1$.

We are interested in traveling wave solutions of equations (3.5). These solutions are functions of only one variable, say $s = x + ct$ with c the (dimensionless) wave velocity. In this context the partial derivatives become ordinary ones.

$$\frac{\partial V}{\partial x} \to \frac{dV}{ds} \equiv \overset{\circ}{V}$$

$$\frac{\partial V}{\partial t} \to c\,\frac{dV}{ds} \equiv c\,\overset{\circ}{V} \tag{3.8}$$

In this notation the F.N. equations are

$$c\,\overset{\circ}{V} = \overset{\circ\circ}{V} - w - f$$

$$c\,\overset{\circ}{w} = \varepsilon(V-\gamma w) \tag{3.9}$$

For fixed values of ε and γ and given function $f(V)$ only certain values of c, called eigenvalues, correspond to solutions with the desired, vanishing behaviour if $|s| \to \infty$. The eigenvalues calculated in practice are of order one. For example Miura [10] calculated,using the values $\varepsilon = 0.08$, $\gamma = 0.8$ and the cubic function $f(V) = 0.33V^3 - 1.20V^2 + 0.44V$, an eigenvalue of $c = 0.81$. To obtain the velocity v in dimensional form we have to use the relation

$$v \equiv (g/2\pi a\, R_a\, c_m^2)^{\frac{1}{2}} \,.\, c \tag{3.10}$$

which can easily be deduced from the transformations (3.4).
For the calculation of this factor we need explicit values of the membrane properties.

In case of unmyelinated animal axons these properties have been measured extensively. In table 1 we quote typical values which should not be associated with a particular species.

symbol	description	typical value
a	(mean) axon radius	5.10^{-6} m
R_a	axoplasm resistance per unit length	$6.4.10^{9}$. $\Omega\ m^{-1}$
$1/R_s$	membrane conductance per unit area	$10\ \Omega^{-1}\ m^{-2}$
c_m	membrane capacitance per unit area	10^2 F m^{-2}

Table 1. Properties of a typical unmyelinated nerve, quoted from ref. [7].

In this table no value for L is specified because it does not directly correspond to a measurable quantity. For fixed values of c_m and g this value should rather be derived from the requirement $\varepsilon << 1$. From the experimental data and assumption (3.7) we find that the result $c = 0.81$ corresponds to a velocity of about 0.6 m/s which agrees well with the order of magnitude observed in unmyelinated axons.

In the case of membranes in the styles of lilies no quantitative experimental data are available yet. In order to estimate the orders of magnitude of the parameters two qualitative features must be taken into account. Firstly, in vegetable cells vacuoles may be present, which at some places may nearly fill up the cell in transversal direction. This may lead to considerable enhancement of the axoplasm resistance R_a. The parameters in the F.N. equations (3.5) and (3.6) are independent of R_a but the calculated velocities scale inversely with the value of R_a. From equation (3.10) we have $v \approx (R_a)^{-\frac{1}{2}}$. It is, however, unlikely that this effect on its own could explain a velocity decrease of some orders of magnitude. Secondly it is found [16] that along the vascular bundles cells with lignified secondary walls are present. To deal with this phenomenon we proceed in two ways, which are separately presented in the next two sections.

§4. Lignification within the Fitzhugh-Nagumo model

In this section we consider the lignified cells in the near vicinity of the membrane as belonging to the membrane and affecting its electrical constants rather than its qualitative electrical behaviour. With this assumption we can still describe the system in terms of the F.N. equations (3.5). The lignified cells will enhance the electrical resistivity of the membrane by a certain amount R_ℓ; see figure 5 for the "implementation" of R_ℓ. Only the part of the F.N. model that is essentially changed is drawn in this figure.

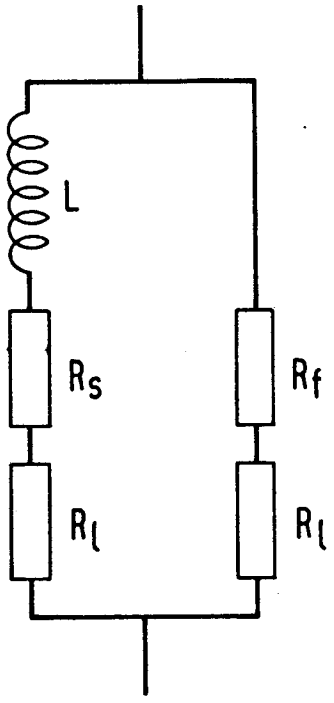

Figure 5. Lignification effects are simulated by adding an extra, linear resistance R_ℓ to the membrane resistance.

It is clear from figure 5 that in the equations this approach is represented by the substitution $R_s \to R_s + R_\ell$. From approximation (3.7) and equation (3.6b) it follows that γ will remain unaffected. For physical reasons ε should also remain the same which can be achieved by adjustment of the L value (equation 3.6a). From equation (3.10) together with assumption (3.7) we obtain the following scaling relation for the velocity.

$$v \approx ((R_s + R_\ell)R_a)^{-\frac{1}{2}} \tag{4.1}$$

If the lignified wall around the vegetable membrane seriously screens it from its surroundings it is reasonable to make the assumption $R_\ell >> R_s$. In that case we have the scaling relation $v \approx (R_a\ R_\ell)^{-\frac{1}{2}}$. From this we conclude that the presence of the lignification and the enhancement of the axoplasm resistance R_a lead to a reduction of wave velocity in the same way. Cumulation of both effects might well explain the considerable difference between animal and vegetable wave velocities.

§5. Lignification within an extended Fitzhugh-Nagumo model

Another approach to lignification effects is to treat the membrane and lignified layer separately. In such a setting the effect of the latter is taken into account by adding an extra resistance R_ℓ to the F.N. model in the way as is drawn in figure 6.

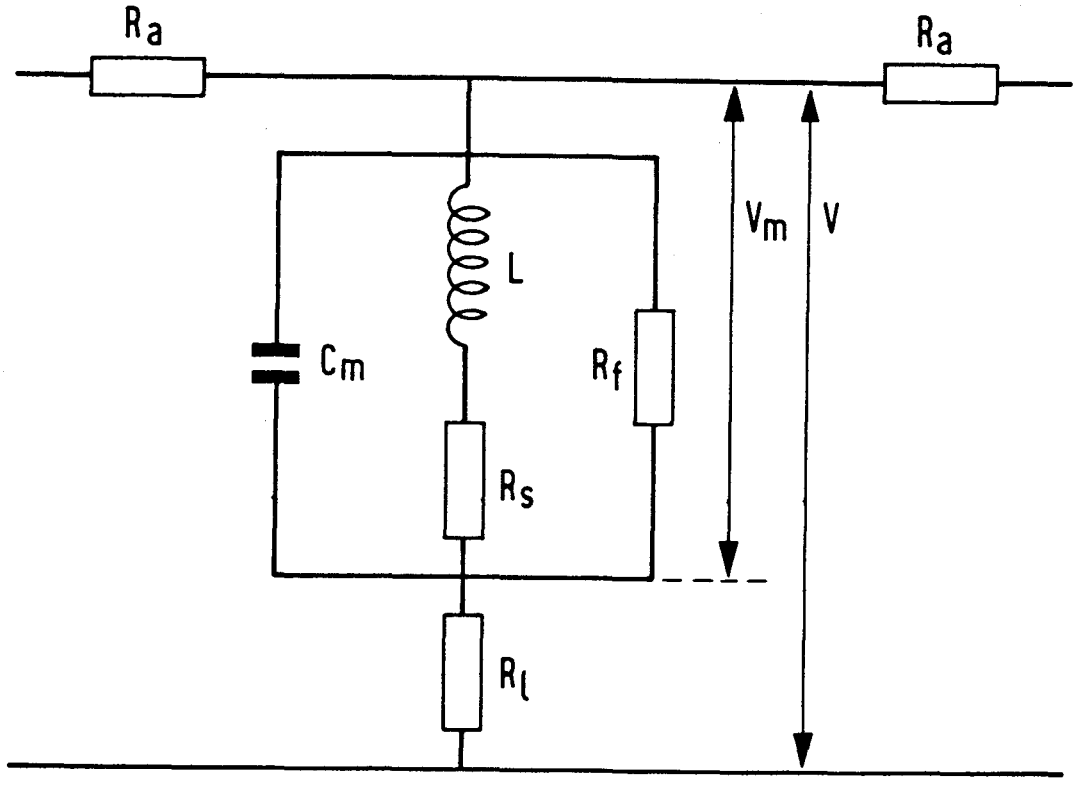

Figure 6. An extra resistance R_ℓ is added to the F.N. model simulating a lignified layer between the membrane and its surroundings.

As denoted in figure 6 we now may discern between the membrane voltage V_m and the voltage V over both the membrane and the lignified layer. Derivation of the corresponding differential equations will be omitted here because the essential steps are already dealt with in section 3. In dimensionless form the equations for traveling wave solutions read as follows.

$$c\,\overset{\circ}{V}_m = \overset{\circ\circ}{V} - w - f \qquad (a)$$

$$c\,\overset{\circ}{w} = \varepsilon(V_m - \gamma w) \qquad (b) \qquad (5.1)$$

$$V = V_m + \beta\,\overset{\circ\circ}{V} \qquad (c)$$

The parameters ε and γ are already defined by (3.6), c is the (dimensionless) velocity and β is defined by

$$\beta = g.R_\ell \qquad (5.2)$$

It is clear that in the limit $\beta \to 0$ equations (5.1) reduce to the F.N. equations (3.9) because then $V \equiv V_m$.
Because it is assumed that the membrane properties are not affected by the presence of the lignified cells the conditions $\varepsilon << 1$ and $\gamma \approx 1$ will still hold as was discussed in section 3. Under these conditions we are interested in the behaviour of the velocity parameter c with increasing β.
In order to find a numerical value for the eigenvalue for a given value of the lignification factor β we used a strategy that is essentially the same as the one suggested by Miura [10].
Since the voltages V and V_m are supposed to vanish for $|s| \to \infty$ the currents w and f do the same. Hence the system of equations (5.1) approaches a linear one for $|s| \to \infty$. We determined the eigenvalues and eigenvectors of the reduced first order linear system by a standard QR routine. It appeared that only one unstable eigenvalue (i.e. with positive real part) existed for the β values of interest. Using a first order perturbation in the corresponding eigendirection from the rest state solution (viz. all variables identically zero) we could find an initial profile for V for the desired solution by guessing values of c and following the solution till we met unrealistic growth either in the positive or in the negative direction. By bisection we managed to update the value of c until the relevant part of the profile was found. In this initial guessing we had a degree of freedom in that any other profile, formed from a given one by translating over a finite distance, is a solution to the problem as well. Once we got a fairly good guess we fixed a certain interval (needed because we had to truncate the range of s) and an attainable value for V at a point

therein. The latter interval condition quaranteed the uniqueness of the numerical solution if only the initial estimate for the profile were accurate enough; moreover it excluded the trivial solution. The system (5.1) was then extended by adding $\overset{\circ}{c} = 0$, making it to a fourth order one. Because of the signs of the real parts of the eigenvalues indicated above, we chose two initial conditions for V and w and one terminal condition for w together with the internal condition resulting in a well conditioned (three point) boundary value problem. It was solved by a collocation solver COLSYS [1] using the previously indicated initial guesses. In this way we found two isolated solitary wave solutions with different values for c. Starting from the voltage profiles obtained in the case of $\beta = 0$ the more complicated system of equations in the case of $\beta \neq 0$ could then be solved. In particular for somewhat larger values of β this led to insurmountable difficulties. Therefore we used an other routine to obtain insight in the inter-dependence of β and c. This routine called AUTO [3] produces bifurcation diagrams for autonomous problems, as far as periodic solutions and Hopf bifurcations are concerned. Since the system under consideration was autonomous it was relatively straight forward to find homoclinic orbits. Also for AUTO we had to truncate the infinite interval to a finite one and in fact we normalized to $[0,\pi]$. In figure 7 we give a plot to show the relation of β and c for the parameter values $\varepsilon = 0.08$ and $\gamma = 0.8$.

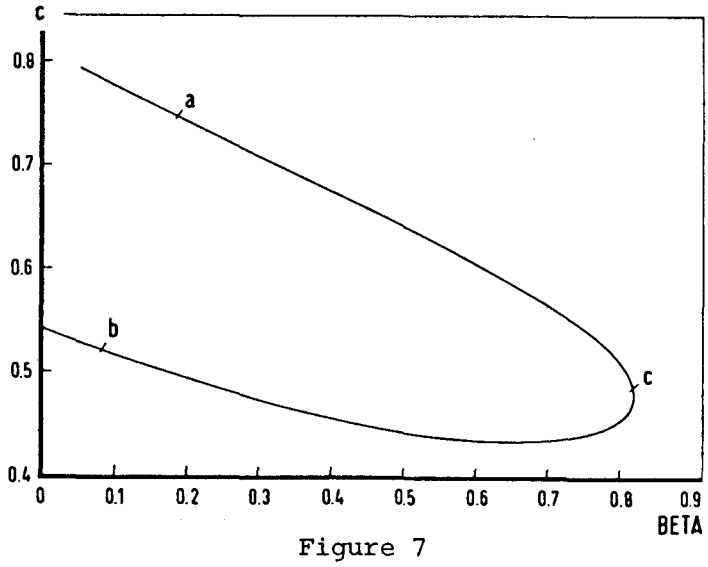

Figure 7

Figure 7. Plot of the eigenvalue c as a function of β for the parameter values $\varepsilon = 0.08$ and $\gamma = 0.8$.

A striking feature of these results is the occurrence of a threshold value $\beta_{max} = 0.81$ (turning point). For $\beta < \beta_{max}$ two solutions exist just as found in the case of $\beta = 0$. If $\beta = \beta_{max}$ one and if $\beta > \beta_{max}$ no traveling wave solutions can be found. In the figures 8, 9 and 10 curves for the respective quantities V, V_m and w are plotted for three typical parameter combinations (c,β). These combinations are taken from figure 7 and in all involved figures denoted by a, b and c. As expected the curves for V and V_m are very similar if β is small (curves 8a, 8b, 9a and 9b) but diverge with increasing value of β (curves 8c and 9c). The V and V_m profiles consist of a single pulse directly followed by a minimum.The latter phenomenon is also characteristic for solutions of the H.H. equations [8,13]. This wave form strongly resembles the bio-electrical response after self-pollination in pistils of lilies (figure 3a).

To investigate the dependence of these results on the value of γ we also used the parameter combination $\gamma = 2.5$ and $\varepsilon = 0.08$. Part of the corresponding (c,β) curve is given in figure 11. Comparing figures 7 and 11 we find that increasing γ yields a decrease of c and an increase of β_{max} by about a factor of two. Increasing β from 0 until β_{max} lowers the c-value. This reduction increases with increasing γ-value and amounts a factor of about 10 in case of $\gamma = 2.5$. Using higher γ-values does not seem to be realistic as explained in section 3 referring to equation (3.7).

Figure 8. Traveling wave profiles of V for three sets of the parameters c and β corresponding to the points a,b and c in figure 7.

Figure 9. Traveling wave profiles of V_m for three sets of the parameters c and β corresponding to the points a,b and c in figure 7.

Figure 10. Traveling wave profiles of w for three sets of the parameters c and β corresponding to the points a,b and c in figure 7.

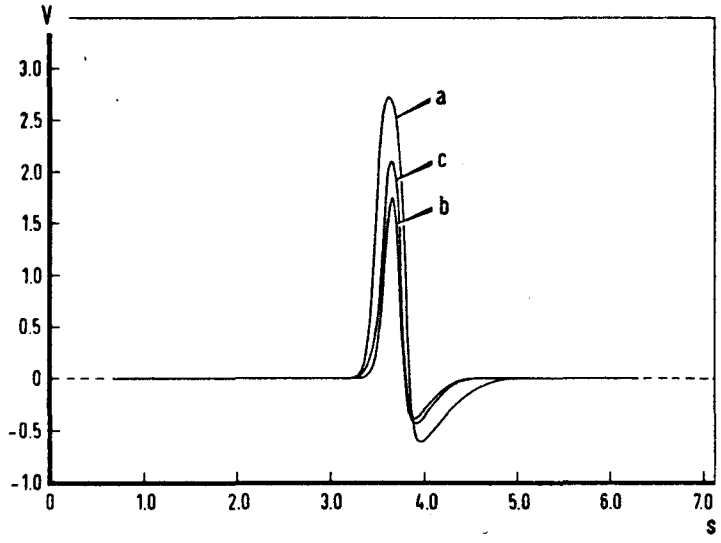

Figure 8.

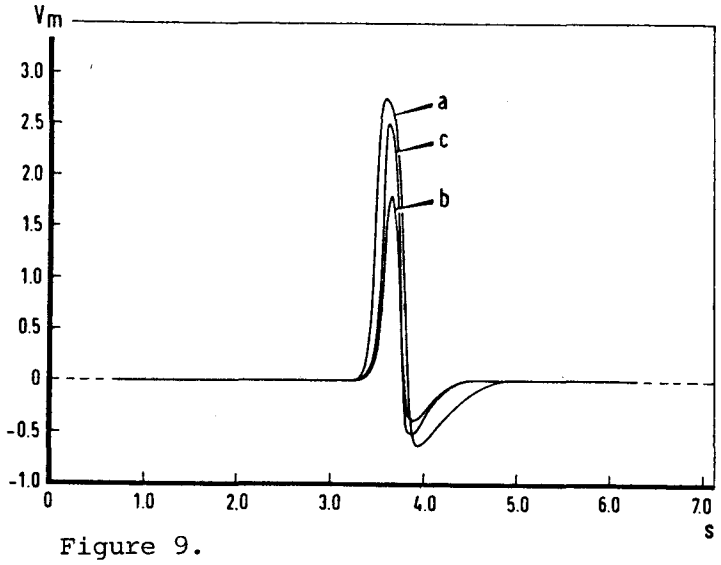

Figure 9.

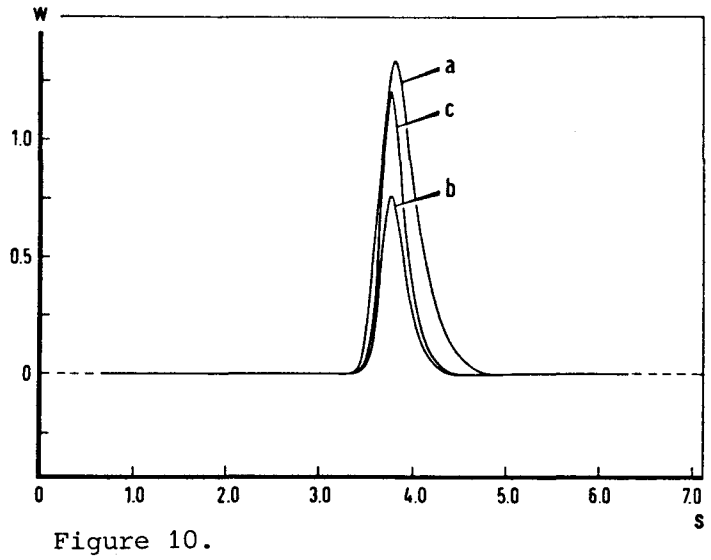

Figure 10.

See page 15 for the captions of figures 8, 9 and 10.

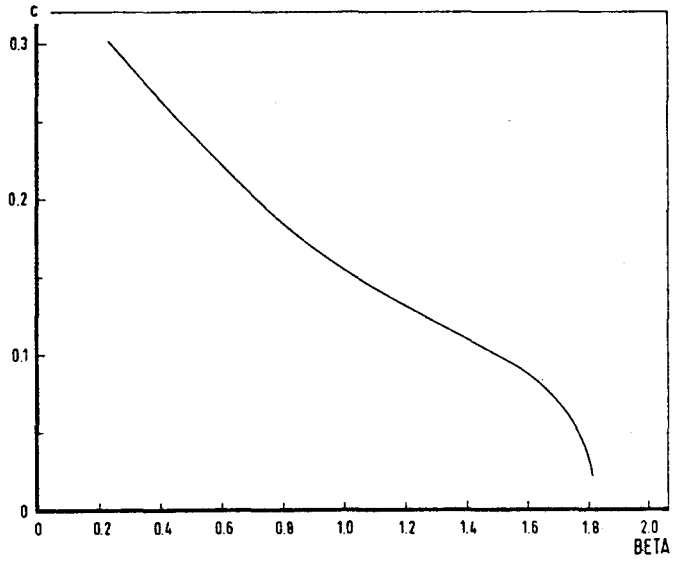

Figure 11. Eigenvalue c as a function of β for the parameter values $\varepsilon = 0.08$, $\gamma = 2.5$.

Assumption (3.7) also provides us with an estimate of the value of β. Combining it with definition (5.2) we obtain the following scaling relation.

$$\beta \approx R_\ell / R_s \tag{5.3}$$

From this relation we conclude that in the case of much lignification ($R_\ell >> R_s$) $\beta >> 1$. Because $\beta_{max} \approx 1$, in this case lignification obstructs the presence of traveling waves. In the case of little lignification, however, the value of β will be in the range $0 < \beta \leq 1$ and, as discussed above, the form and velocity of the traveling waves only differ in a minor way from the results calculated without accounting for lignification ($\beta \equiv 0$). So we conclude that, if the approach presented in this section would describe lignification effects well, this phenomenon on its own could not explain the low velocities observed in plants.

§6. Concluding remarks

The bioelectric responses in pistils of lilies after self- and cross-pollination of the stigma (figures 3a and b) can be simulated using the Hodgkin-Huxley model, which, until now, has only been applied to human and animal nerves. This indicates that vegetable membranes are controlled by the same kind of processes as are known for the nerve system. To obtain the characteristic "plateau" solutions found in case of cross-pollination (figure 3b) two relatively slow subprocesses should take place (e.g. K and Ca activation) in the membrane which differ considerably in velocities.

In order to explain the velocity range of the signals (cm/h) we explored the Fitzhugh-Nagumo model in two ways. First we simulated the effect of lignification by a lowering of the permeability of the membrane for all ion currents present. In this way it is shown that the velocity of traveling waves inversely scales with the amount of lignification. As explained in section 3, it also inversely scales with the axoplasm resistance, which may be enhanced considerably in vegetable membranes due to the presence of vacuoles. Cumulation of both effects could well explain the very low velocities observed. We also tried to account for lignification by extending the model and introducing an extra resistance branch. In this way the membrane and the lignified layer are treated separately. It is found that, if $R_\ell >> R_s$, with R_ℓ the lignification resistance and R_s the membrane resistance for ion processes, the model does not possess traveling wave solutions. Too much lignification apparently prohibits any signal in this description. In the range $0 \leq R_\ell \leq R_s$ traveling waves solutions exist. By increasing the value of R_ℓ in this range we decrease the wave velocity by at most a factor of ten. So we conclude that either the low order of magnitude of wave velocities is not due to lignification or this is not the right way to account for this phenomenon.
Because in principle the Hodgkin-Huxley and Fitzhugh-Nagumo models are suitable to describe both the form and velocities of the measured bio-electrical responses it is certainly worthwhile to determine the membrane parameters in styles of flowers in more detail. It is clear from the analyses presented here that drawing more definite conclusions from the models we used should require to investigate which ele-

ments play a role in the electric household of the vascular bundles and the relative velocities of the (in)activation processes of these elements. Another important parameter, which should be measured, is the resistance of the axoplasm in vegetable membranes. Further the position and resistance of the lignified cells should be studied in more detail.

References

1) Ascher, U., Christiansen, J. and Russell, R.D., COLSYS - a collocation code for boundary value problems, Lecture Notes in Computer Science 76, Springer-Verlag, Berlin, 164-185 (1979).

2) Carpenter, G.A. A geometric approach to singular perturbation problems with applications to nerve impulse equations. J. of Differential Equations 23,335-367, (1977).

3) Doedel, E.J., AUTO - a program for the automatic bifurcation analysis of autonomous systems, Cong. Num. 30, 265-284, (1981).

4) Fitzhugh, R. Thresholds and plateaus in the Hodgkin-Huxley nerve equations. J. Gen. Physiol., 43, 867-896, (1960).

5) Fitzhugh, R. In: Biological engineering (Schwan, H.P., ed.) Mathematical models of excitation and propagation in nerve, pp 1-85. New York: Mc Graw-Hill. (1969).

6) Fitzhugh, R. Dimensional analysis of nerve models. J. Theor. Biol., 40, 517-541, (1973).

7) Hobbie, R.K. Intermediate Physics for Medicine and Biology, John Wiley and Sons, New York, 1978, chapter 6.

8) Hodgkin, A.L., Huxley, A.F. A quantitative description of membrane current and its application to conduction and excitation in nerve. J. of Physiology (London), 117, 500-544, (1952).

9) Linskens, H.F., Spanjers, A.W. Changes of the electrical potential in the transmitting tissue of Petunia-styles after cross- and self-pollination. Incomp. Newsletter 3, 81-85 (1973).

10) Miura,R.M. Accurate computation of the stable solitary wave for the Fitzhugh-Nagumo equations. J. Math. Biology, 13, 247-269, (1982).

11) Nagumo, J., Arimoto, S., Yoshizawa, S. An active pulse transmission line simulating nerve axon. Proc. IRE, 50, 2061-2070, (1964).

12) Rinzel, J., Keller, J.B. Traveling wave solutions of a nerve conduction equation. Biophys. J. 13, 1313-1337 (1973).

13) Scott, A.C. The electrophysics of a nerve fiber. Rev. Mod. Phys. 47, 487-533 (1975).

14) Sinyukhin, A.M. Britikov, E.A. Generation of potentials in the pistil of Incarvillea and Lily in conjunction with movement of the stigma and fertilization.Sovjet Plant Physiol. 14, 393-403 (1967).

15) Spanjers, A.W. Bioelectric potential changes in the style of Lilium longiflorum after self- and cross-pollination of the stigma. Planta 153, 1-5, (1981).

16) Spanjers, A.W., Pierson, E.S. Lignified cells in Lilium longiflorum Thunb. styles and their relation to bioelectric potential changes. Planta, 156, 193-198, (1982).